ISBN: 978-3-95450-192-2 doi:10.18429/JACoW-IBIC2017-WE2AB3

A NANOFABRICATED WIRESCANNER: DESIGN, FABRICATION AND EXPERIMENTAL RESULTS

M. Veronese*, S. Grulja, G. Penco, M. Ferianis, Elettra-Sincrotrone Trieste, Trieste, Italy
S. Dal Zilio, S. Greco[1], M. Lazzarino, IOM-CNR Laboratorio TASC, Basovizza, Trieste, Italy
L. Fröhlich, Deutsches Elektronen-Synchrotron DESY, Hamburg, Germany
[1] also at Graduate School of Nanotechnology, University of Trieste, P.le Europa 1, Trieste, Italy

Abstract

Measuring the transverse size of electron beams is of crucial importance in modern accelerators, from large colliders to free electron lasers to storage rings. For this reason several kind of diagnostics have been developed such as: optical transition radiation screens, scintillating screens, laser scanners and wirescanners. The last ones although providing only a multishot profile in one plane have proven capable of very high resolution. Wirescanners employ thin wires with typical thickness of the order of tens of microns that are scanner across the beam, whilst ionizing radiation generated from the impact of the electrons with the wires is detected. In this paper we describe a new approach to wirescanners design based on nanofabrication technologies. This approach opens up new possibilities in term of wires shape, size, material and thickness with potential for even higher resolution and increase flexibility for instrumentation designers. We describe the device, the fabrication process and report measurement performed on the FERMI FEL electron beam.

INTRODUCTION

It is of importance for a wide variety of accelerators to have accurate control of machine optics to reach the desired high electron densities. This task is accomplished with the help of transverse profile instrumentation. Through the decades several concepts of transverse profile instrumentation has been explored depending on the specific parameters of the accelerator and the resolution requirements. Two of the most extensively deployed in electron accelerators are imaging screens and wirescanners (WSC). The imaging screens are capable of providing a two dimensional profile in a single shot but have resolution hardly better than 10 µm (scintillator screens) [1]. In the case of a metallic screen emitting transition radiation they may be plagued by coherent optical transition radiation (COTR) [2]. The wirescanners on the other side can provide only one dimensional multishot measurement of the profiles but can reach better resolution than screens. Typical WSC detection is based on measurement of the ionizing radiation dose produced by the electron beam hitting the wires. For high brightness electron beams where the beam sizes are below 100 µm, the wirescanner designer has the possibility to choose amongst wires of different materials, such as: tungsten, aluminum and carbon [3–5], and wire diameter to reach the needed compromise between signal, resolution and mechanical robustness. For a detection based on ionizing radiation the larger the atomic number and density of the material the larger the signal. The mechanical robustness of the wires equipped diagnostics is mostly related to the vibrations induced by the motorized actuator used for the scan while beam induced heating may be an issue mainly for high repetition rate machines. The resolution of a measurement performed with a wire of diameter d corresponds to the r.m.s. of the cylindrical distribution i.e. $d/4$ [5]. In practice the diameter of the wire is typically limited to about 5 µm. In this paper we describe a novel device manufactured using nanofabrication techniques providing several potential benefits in terms of instrumentation design including the potential for sub-micron resolution.

DEVICE DESIGN

The basic idea is to create thin bridges across a robust frame. By nanofabrication these structures can be made thinner and narrower than a traditional wire. For this purpose we use a silicon substrate (thickness 500 µm) coated by 2 µm low stress silicon nitride (SiN) film. After the patterning the SiN coating with suitable structures, the etching of the substrate allowed the release of suspended structures bridged on a 3x9 mm free window. The structures made in this way have a rectangular cross section and from now on we will refer to them as nanofabricated wires (NF wires). Their width w determines the resolution. It can be demonstrated that the r.m.s. of a rectangular distribution is $w/\sqrt{12}$. With nanofabrication the width can made as small as 0.5 µm and thus the resolution can potentially reach 0.15 µm. The energy loss per unit thickness of a high energy electron beam scales with the square of the atomic number Z of the target material and is linear in its density ρ [6]. While in general more signal is better, for potential applications such as intra undulator diagnostics having a lower ionizing dose is a beneficial property. SiN has a low density of $\rho(Si)$ =3 gcm^{-3}). Considering $Z(Si)$ = 14 and that $Z(N)$ = 7 an effective atomic number can be calculated for SiN according to [7] to be $Z(SiN)$ = 12.5. on the basis of this two quantities a first approximation of the relative yield between wires can be calculated. Considering for example a NF wire of width of 10 µm and a thickness of 2 µm the dose generated by a 2x10 µm SiN NF wires is calculated to be 929 times less the one generated by a 10 µm tungsten wire ($Z(W)$ = 74, $\rho(W)$ =19.35 gcm^{-3}).A comparison between cylindrical wires and NF wires can be found in Table 1. A benefit of the NF wires compared to a traditional

* marco.veronese@elettra.eu

ISBN: 978-3-95450-192-2 doi:10.18429/JACoW-IBIC2017-WE2AB3

wires is that the ionizing yield can be chosen independently from the desired resolution. In our device, for example, we made a coating of silver with thickness of 0.5 µm on both sides of the device. The Ag film increases the device dose emission of about an order of magnitude without changing the resolution.

Table 1: Relative Ionizing Radiation Dose of Wires

Type	Dimensions	Material	Rel. Yield
Wire	10 µm	W	929
Wire	5 µm	Al	1
Bridge	0.5/2/0.5x10 µm	Ag/SiN/Ag	26.7
Bridge	2x10 µm	SiN	0.84

IONIZING RADIATION SIMULATIONS

A simulation with the Monte Carlo particle tracking code Fluka [8, 9] has been performed to compare the radiation field created by the four wire types described in Table 1. The simulation contains exclusively electromagnetic interactions and tracks electrons and positrons down to a kinetic energy of 20 keV, photons down to 5 keV. The simulated electron beam has a Gaussian profile of σ =50 µm and no divergence. It hits the wire centrally at z=0. For the sake of simplicity, the rest of the simulation space is empty (vacuum). The first relevant finding is that the electron and not the photons are dominating the ionizing radiation dose. This means that the approximation used in Table 1 is not valid. A second aspect is related to the amplitude of the cross sections involved which is small. This means that also the divergence of the ionizing shower of primary electrons is small. to better understand all the relevant aspects of dose emission simulations have been carried out. The Figure 1 depicts the equivalent dose delivered in the plane orthogonal to the electron beam and set at 10 meters downstream the impact point. The simulation evaluates almost the same dose for 2 µm SiN NF wire vs the 5 µm Aluminum wire. It predicts 7.5 time higher dose for the Ag/Si/Ag NS wire and about 175 times higher dose for the 10 µm tungsten wire.

DEVICE FABRICATION AND CHARACTERIZATION

The device used in the experiment has been fabricated at IOM-CNR Laboratory in Trieste. The fabrication process has been completed starting from a double polished Silicon wafer substrate (500 um thickness) coated by LDCVD low stress SiN film (2000 nm) and DC Sputtered chromium (100 nm). Suitable pattern has been produced on coated optical resist (MEGAPOSIT SPR220 1.2) by classical UV lithography process, defining on one side the windowing structure and, on the other one, the bridged wires. Following wet etching protocol allowed to reproduced the pattern on the Cr thin film, exploited as a mask for high aspect ratio dry etching ICP-RIE process for the removal of exposed SiN layer. The sample have been transferred in KOH wet etchant

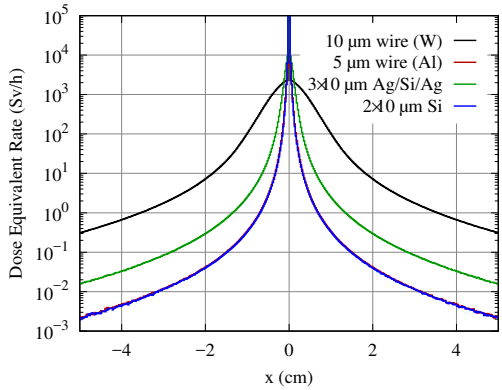

Figure 1: Cross sectional distribution of ionizing radiation dose for different wires at a distance of 10 meters from the impact point.

solution (33% in wt, 75°C) in order to selectively remove the Si substrate and complete the release of the suspended SiN wire. Well set protocol has been implemented in order to dry the samples avoiding the damage of obtained structures. The following metal coating step has been performed by thermal metal evaporation of selected material: in order to reduce the stress induced by metal film, the deposition has been done on both the device sides. The fabrication process just described was applied to obtain suitable for a proof of principle test. For this test only the horizontal projection of the bunch transverse profile was of interest. For this purpose the device was fabricated with five parallel bridges each at a distance of 1.5 mm from the other. The length of the bridges are 3 mm and their width is: 20.6 µm, 13.5 µm, 6.7 µm, 4.5 µm. The larger bridges were intended for initial setup of the measurement. While the thinner for performance assessment.

In Figure 2 a scanning electron microscope (SEM) image of a 10 µm bridge is reported to show the high quality of the fabrication process.

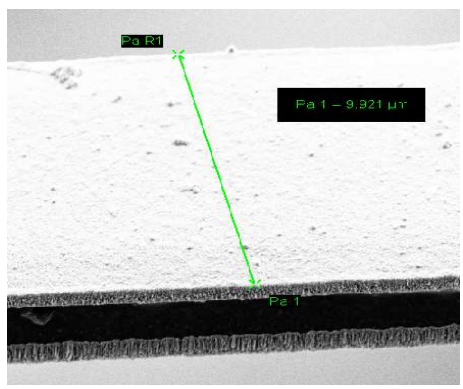

Figure 2: Scanning electron image of a 9.9 µm NF wire.

EXPERIMENTAL SETUP

The experiment was conducted at the FERMI FEL in Trieste (Italy) [10]. The device described in the previous section

ISBN: 978-3-95450-192-2 doi:10.18429/JACoW-IBIC2017-WE2AB3

was installed in the intra undulator imaging screen n.4 of the FEL1 undulator chain [11]. The main reason for this choice is the in situ capability of comparison with high resolution screen, the availability of a motorized actuator fitted with independent optical encoder for wire scanning and the availability of ionizing radiation detectors. Moreover both the high energy and the low beta optics in this machine position produce electron beam sizes of the order of 100 µm that are ideal for the measurements. Finally the chosen location was also suitable for an initial evaluation of compatibility of such a device with the operation of the accelerator for what concerns the damage to the undulators. During the experiment the FERMI beam charge was of 700 pC, and the energy of 1.285 GeV. Figure 3 shows a layout of the FERMI FEL1 area involved in the experiment. The ionizing radiation detectors installed in the FELs region are of two types: Cherenkov fibers and ionization chambers. They are part of the machine protection system (MPS) of FERMI [12] and were used as measurement devices. The Cherenkov fibers run along the entire undulator vacuum chamber. The light produced by high energy particles hitting the fiber is transferred out of the tunnel to an optical to electrical conversion unit based on MPPC detector. The electrical signal is then acquired by means of a VME ADC board with 12 bits resolution and 250 Msamples/s sample rate. The ionization chambers are installed in the vicinity of each imaging screen chamber. The ionization chambers are filled with air at atmospheric pressure and connected to the controller which supplies the high voltage (1 KV) and acquires the signal via an embedded picoammeters. The ionizing chamber (IC4, Ic5 and IC6) are depicted in figure as green rectangles. As an addition for the experiment we installed a spool of Cherenkov fibers at about 12 meters downstream the NF wires.

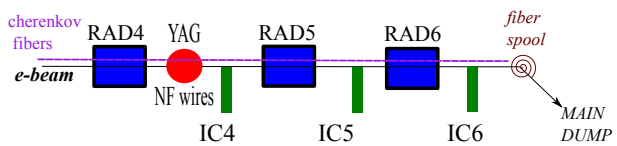

Figure 3: Experimental layout. The ionizing chamber are in green. The imaging screen diagnostics chamber containing the YAG and the NF device are depicted as red circle. The FEL radiators are in blue.

MEASUREMENT RESULTS

The signal detected from the ionizing shower induced by the NF wires is rather small. To obtain the best signal to noise ratio, we took care that both optics and trajectory in FEL1 were optimal, to avoid any beam scrapering which would cause a background in our measurements. Considering a vertical beam size of 100 µm this means that the vertical aperture of 3 mm is about 30 times the vertical size. So no core electrons are expected to contribute to the background. On the other side vertical halos due to wakefields may become relevant. The signal from the halos can potentially become of the same magnitude of a 10 µm wire if the halo size is so large to hit the frame. We took care during the measurements to verify that the contribution from the halos was suppressed. Figure 4 shows the beam losses signal measured by the Cherenkov fibers, while scanning the NF wires position with a step of about 25 µm. The scanning step was chosen in relationship with the expected beam spot size of few hundred microns. Each data point plotted in the figure corresponds to the average over five consecutive shots and the error bars are the standard deviation. Concerning

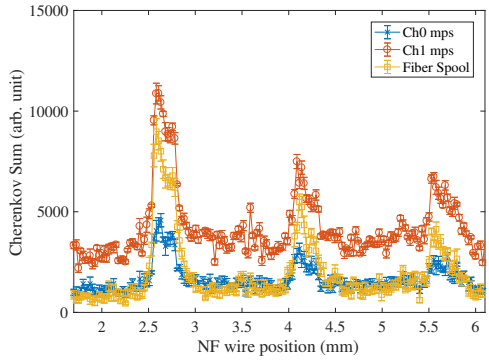

Figure 4: Beam losses signal from three wires acquired by the Cherenkov fibers diagnostics.

the Cherenkov fibers, we report the peak and the integrated signal for each wire position. Figure 5 shows the beam losses signal measured by the Ionization Chambers IC4, IC5 and IC6. The different signal amplitudes derived from each wire

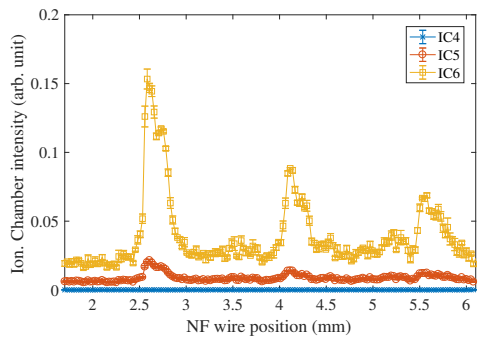

Figure 5: Beam losses signal from the ionization chambers during the wire scan.

depend only on the width of the wires. The IC6 and the fiber spool signals have a comparable SNR which is better than the other detector. The difference in the relative amplitude of the ionization chambers depends on the position of the chamber with respect to the NF wire which is located in the same position of IC4. IC5 which is located 3.7 meters downstream the wires shows a detectable signal but IC6 which is located at 7.4 meters shows maximum signal. The measured beam spot size measurement obtained analyzing the data in the above figures is in good agreement between detectors. For example considering the 20.6 µm NF wire the measured electron beam size is 129 µm ± 6 µm). Being a proof of principle experiment we wanted to compare a profile measured

ISBN: 978-3-95450-192-2 doi:10.18429/JACoW-IBIC2017-WE2AB3

from the nanofabricated device against our imaging high resolution scintillating screen. These imaging screens employ a COTR immune detection geometric and they are capable of measuring beam sizes down to 15 µm [11]. Figure 6 shows the horizontal profile of the electron beam obtained with the nanofabricated 13.5 µm wire averaging step by step over 20 consecutive shots. Figure 7 the electron beam transverse

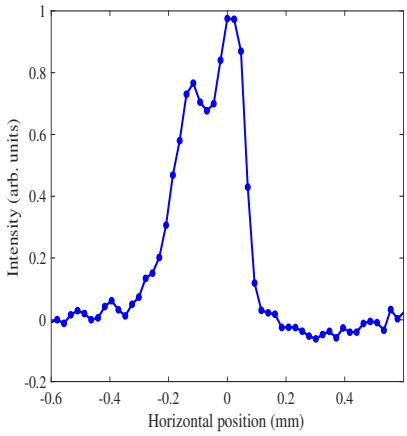

Figure 6: Horizontal profile obtained with the 13.5 µm NF wire.

image from the IUFEL imaging system is reported. The

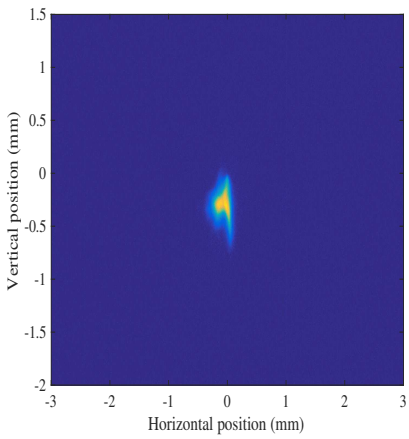

Figure 7: Comparison of nanofabricated wire profile with double gaussian function.

beam sizes obtained by the wire and the screen are in very very good agreement.

CONCLUSIONS AND PERSPECTIVES

We have reported the design, fabrication and proof of principle experiment of a wire scanner based on a nanofabricated device. The experimental data of the transverse been profile obtained with such device show good agreement with the high resolution scintillating imaging screen diagnostics. The technology underling this device offers potentially higher resolution, more flexibility and ease of installation compared to traditional wire scanners. The device is best suited for high brightness electron beams with beam size smaller than a few hundred microns. A technological limitation is the size of the aperture obtainable along the wire length to avoid breaking the bridges which cannot be higher than 3-4 mm. A single device with 2 wires at 90 deg with each other that is moved into the beam at 45 deg with the wires can be manufactured leading to a very compact wirescanner diagnostics. Application to photon sources from UV to soft X-ray is feasible by measuring the photo-ionization current. Application to FELs is also possible if the photon densities involved are below the damage threshold.

REFERENCES

[1] M. Yan *et al.*, in *Proc. DIPAC2011*, Hamburg, Germany. pp. 440–442 (2011).

[2] R. Akre, D. Dowell, P. Emma, J. Frisch, S. Gilevich, *et al.*, *Phys. Rev. ST Accel. Beams* 11 (2008), 030703.

[3] H.-D. Nuhn *et al.*, Report No. SlAC-PUB-19098, 2006.

[4] U.Hahn *et al.*, *Nucl. Instrum. Methods Phys. Res Sect.* A, 592, 189, (2008)

[5] G. Orlandi *et al.*, *Physical review Accelerator and Beams*, 19, 092802, (2016).

[6] R.C. Fernow, "Introduction to Experimental Particle Physics", Cambridge University Press, Cambridge, England, (1986).

[7] R. C. Murty, *Nature* 207, 398-399 (24 July 1965)

[8] T. T. Böhlen, F. Cerutti, M. P. W. Chin, A. Fassò, A. Ferrari, P.G. Ortega, A. Mairani, P. R. Sala, G. Smirnov, and V. Vlachoudis, "The FLUKA Code: Developments and Challenges for High Energy and Medical Applications", *Nuclear Data Sheets* 120, 211-214 (2014)

[9] A. Ferrari, P.R. Sala, A. Fassó, and J. Ranft, "FLUKA: a multi-particle transport code", CERN-2005-10 (2005), INFN/TC-05/11, SLAC-R-773

[10] C. Bocchetta *et al.*, FERMi@Elettra Conceptual Design Report, Tech Report No. ST/F-TN-07/12, 2007.

[11] M. Veronese *et al.*, in *Proc. IBIC2012*, pp. 519-523, Tsukuba, Japan, August 2012.

[12] L. Fröhlich *et al.*, in *Proc. FEL'10*, pp. 667-670, Malmö, Sweden, August 2010.